

## Piezoelectric energy harvesting from rail track vibration using frequency up-conversion mechanism

Guansong Shan\*, Yang Kuang\*, Meiling Zhu\*

\* College of Engineering, Mathematics and Physical Sciences,  
University of Exeter, Exeter EX4 4QF, UK

(e-mail: [gs573@exeter.ac.uk](mailto:gs573@exeter.ac.uk), [y.kuang@exeter.ac.uk](mailto:y.kuang@exeter.ac.uk), [m.zhu@exeter.ac.uk](mailto:m.zhu@exeter.ac.uk))

**Abstract:** Piezoelectric energy harvesting has great powering potential in railway applications, but current piezoelectric literature for rail track vibration mainly focuses on a single piezoelectric element or piezoelectric cantilever, whose output power is usually at the level of  $\mu\text{W}$ . In this work, a piezo stack energy harvester using the frequency up-conversion method with attractive magnetic force is proposed and experimentally validated for harvesting energy from rail track vibration. It consists of two parts, an inertial mass system and a piezo stack system. The frequency up-conversion mechanism is realised by allowing the inertial mass to attach and detach the piezo stack transducer periodically with the help of the attractive magnetic force. The attractive magnetic force contributes to the collision between the two systems, especially when the excitation frequency is near the resonant frequency. A theoretical model of the proposed energy harvester considering the colliding motion and magnetic force is established. A prototype is fabricated and can generate a peak power of 96.69 mW and average power of 2.59 mW at an input acceleration of 1 g applied at 9 Hz with an optimum load impedance of 200  $\Omega$ .

Copyright © 2022 The Authors. This is an open access article under the CC BY-NC-ND license (<https://creativecommons.org/licenses/by-nc-nd/4.0/>)

**Keywords:** Piezoelectric energy harvesting, Rail track vibration, Frequency up-conversion mechanism; Piezo stack, Mechanical transformer.

### 1. INTRODUCTION

Rail transportation systems are essential to society. To monitor rail infrastructures in real-time and detect faults before they cause any damage, condition monitoring based on wireless sensor networks (WSNs) has attracted great attention due to their excellent flexibility and low installation cost. However, one major challenge with WSNs is the power source. Conventional batteries have a very limited lifetime. Replacing or recharging batteries can be difficult when the sensor nodes are distributed in a large area and large number. In this regard, energy harvesting provides a promising solution by converting the ambient energy sources to supply the WSNs.

Vibration energy is a promising energy source for power harvesting in the railway field because it is easy and convenient to get when the train passes by, and it possesses enormous powering potential. It was reported that the average vibration energy level decreases from the top to the bottom of the track structure due to the energy stored and consumed in each part (Jiang and Gao, 2020). As a result, we focus on the rail track other than the sleeper as the vibration source in this paper. Train induced track vibration varies in amplitude and frequency depending on rail types, track foundations, trainloads and velocities, the separation between wheelsets, and even the maintenance history of the track. However, it was reported that when the frequency of the vertical track vibration is below 30 Hz, the quasi-static moving axle load is the main reason for track vibration, independent of vehicle and track dynamics (Sheng et al., 2003) (Cleante et al.,

2019). Therefore, this frequency region is of interest in this paper.

Electromagnetic and piezoelectric mechanisms are of particular interest in railway vibration energy harvesting due to their higher electromechanical coupling capability, simple design, and without the need of an initial external voltage source (Cao et al., 2019) (Fan et al., 2018). Electromagnetic energy harvesters are based on the principle of Faraday's law of electromagnetic induction. A linear type with a typical moving magnet and fixed coil design was demonstrated to harvest rail track vibration-induced energy by Gao et al. (Gao et al., 2016a). When the rail track deflects, the permanent magnet vibrates under the restriction of a mechanical spring, and the coil will generate voltage due to the changing magnetic field. To guarantee better electromagnetic compatibility and improve the energy harvesting performance, a combination of moving coil and fixed magnet (Bradai et al., 2018), and moving magnets and moving coils (Liao et al., 2015) were developed. Different from the linear type, the proof mass is connected to the frame by a magnetically levitated suspension instead of traditional mechanical springs in the typical nonlinear design (De Pasquale et al., 2012). The magnetic suspension is created by introducing two permanent magnets attached to the basement to produce a repulsive force on the levitating magnet. Compared to the linear type, the nonlinear levitation type can broaden the frequency bandwidth. Another electromagnetic railway energy harvester type is the gear-based harvester (Pan et al., 2019), which generally consists of motion conversion structures, gear drives, and a generator. The gear-based electromagnetic railway energy harvester can harvest

energy in the range of W, but the mechanical efficiency is typically low because of the energy losses in the complex transmission (Bosso et al., 2020) and the volume of the gear-based energy harvester is generally large.

Piezoelectric energy harvester presents numerous advantages including high energy and power density, simple structure, good scalability, ease of application, and versatile shapes (Covaci and Gontean, 2020). Attaching a small piezoelectric element to the underside of the rail was first presented (Nelson et al., 2008) (Cahill et al., 2014), but the generated power is unsatisfying. Moreover, A cantilever with a proof mass at its free end and piezoelectric material attached to it is the simplest and most common structure used in vibration piezoelectric energy harvesters. For example, A PZT cantilever was attached to the rail track and generated a peak output power of 4.9 mW with a load impedance of 100 k $\Omega$  at rail acceleration of 5 g and a frequency of 7 Hz in the lab (Gao et al., 2016b). Compression modes of piezoelectric materials were also investigated due to their higher coupling factor. Wang et al. (Wang et al., 2015) simulated the piezoelectric stack device installed at the bottom of the rail utilizing the compression mode of piezoelectric materials and the results showed the maximum total energy produced was 21.88 mJ. It demonstrates that the output using a piezoelectric stack alone is unsatisfying.

Therefore, in this work, we present a piezo stack transducer consisting of a mechanical transformer and a piezo stack applied to the rail track vibration to improve the energy harvesting performance. To harvest the low frequency vibration of rail track, the frequency up-conversion mechanism achieved by attractive magnetic force is investigated. This paper is organized as follows. Section 2 introduces the design and modelling of the proposed energy harvester. Section 3 describes the fabricated prototype of the harvester and the experimental results. Finally, conclusions are drawn according to the relevant analysis.

## 2. PROPOSED PIEZOELECTRIC ENERGY HARVESTER

Fig. 1 illustrates the schematic of the proposed energy harvester based on the frequency up-conversion mechanism achieved by an attractive magnetic force. It consists of two parts, a mass system and a piezo stack system. The mass system comprises an inertial mass, a spring, and a permanent magnet. The resonant frequency of the mass system is designed to be the dominant frequency of the rail track vibration (9 Hz). The piezo stack system is a piezo stack transducer with a ferritic steel stud at its top. The ferritic steel stud interacts with the magnet and transfers the magnetic force to the mechanical transformer, which then amplifies and redirects this vertical force to a horizontal one and applies to the piezo stack operating in  $d_{33}$  coupling mode. The stud is used to control the magnitude of the magnetic force and ensure a relatively large contacting surface area between the piezo stack transducer and permanent magnet when the collision occurs.

Fig. 2 shows the frequency up-conversion mechanism achieved by attractive magnetic force in the proposed energy harvester. When the rail track vibrates, the inertial mass

together with the permanent magnet are actuated to oscillate. As the magnet travels downwards and approaches the piezo stack system, the magnetic force between the magnet and the stud increases, as shown in Step 1. When the displacement or the magnetic force is large enough, the stud is attached to the magnet with a collision, as shown in Step 2. As the magnet travels upwards and away from the piezo system, the magnet and the stud are separated, leading to free vibration of the piezo stack transducer., as shown in Step 3. In this way, the low frequency vibration is converted to the high frequency resonance of the piezo stack transducer, resulting in increased power output. A schematic showing a potential installation of the energy harvester is exhibited in Fig. 3.

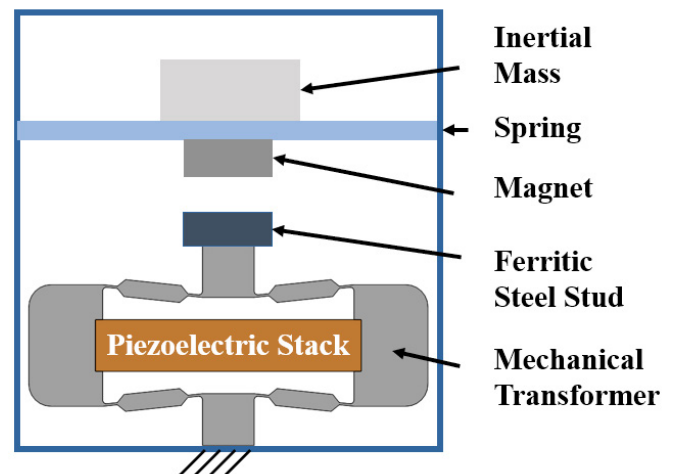


Fig. 1. Schematic of the proposed energy harvester with attractive magnetic force.

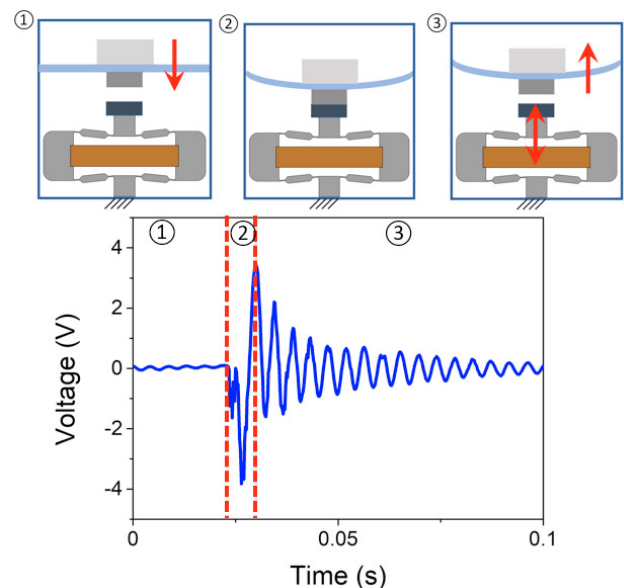


Fig. 2 Schematic showing frequency up-conversion mechanism achieved by attractive magnetic force in the proposed energy harvester.

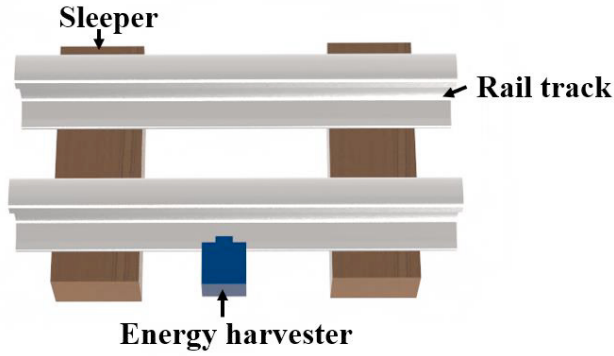


Fig. 3. A schematic showing a potential installation of the energy harvester.

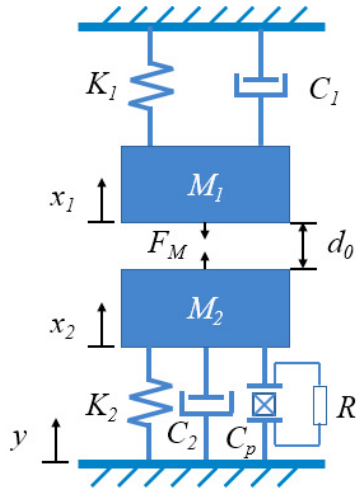


Fig. 4. Simplified analytical model of the proposed energy harvester.

The energy harvester can be mechanically modelled as two mass–spring–damper systems that influence each other as shown in Fig. 4. It can be divided into two states in terms of its dynamic behaviour.

State 1: No collision occurs and the two systems vibrate separately ( $x_1 - x_2 + d_0 > 0$ ).  $x_1$  and  $x_2$  are the displacements of the mass system and the piezo stack system respectively;  $d_0$  is the initial interval between the magnet and ferritic steel.

State 2: Inertial mass is latched onto the transducer ( $x_1 - x_2 + d_0 \leq 0$ ).

Considering the dynamics of state 1, we characterize the motion of the two systems as two second-order differential equations (1, 2).

$$M_1 \ddot{x}_1 + C_1 \dot{x}_1 + K_1 x_1 = -M_1 \ddot{y} + F_M \quad (1)$$

$$M_2 \ddot{x}_2 + C_2 \dot{x}_2 + K_2 x_2 - \alpha V = -M_2 \ddot{y} + F_M \quad (2)$$

where  $M_1$  is the total mass of the inertial mass and magnet;  $M_2$  is the total mass of the piezo stack transducer and ferritic steel;  $C_1$  and  $C_2$ ,  $K_1$  and  $K_2$  are the damping coefficients,

stiffness of the mass system and the piezo stack system respectively (subscript 1 represents the mass system while subscript 2 stands for the piezo stack system);  $V$  represents voltage;  $\alpha$  is the electromechanical coupling coefficient of the piezo stack;  $y$  represents the input displacement;  $F_M$  stands for the magnetic force between the piezo stack system and the magnet.

When the inertial mass attaches to the piezo stack system (State 2), the motion of the coupled system is given by the following equation.

$$(M_1 + M_2) \ddot{x} + (C_1 + C_2) \dot{x} + K_2 x + K_1 (x + d_0) = -(M_1 + M_2) \ddot{y} \quad (3)$$

where  $x$  is the displacement of the inertial mass and piezo stack transducer.

When the mass system collides with the piezo stack system ( $x_1 - x_2 + d_0 \leq 0$ ), some energy is lost from the ensuing collision. The impact between the two systems can be modelled as an elastic collision (Galchev et al., 2011) and the velocities of the two systems are given by the following equations

$$v_1 = \frac{(C_R + 1)M_2 u_2 + (M_1 - C_R M_2) u_1}{M_1 + M_2} \quad (4)$$

$$v_2 = \frac{(C_R + 1)M_1 u_1 + (M_2 - C_R M_1) u_2}{M_1 + M_2} \quad (5)$$

where  $u_i$  and  $v_i$  are the velocities of the mass before and after the collision.  $C_R$  is the coefficient of restitution of the materials coming into contact.

The electrical equation can be attained as

$$C_p \dot{V} + \frac{V}{R_L} + \alpha \dot{x}_2 = 0 \quad (6)$$

where  $C_p$  is the equivalent capacitance of the piezoelectric stack and  $R_L$  is the external resistance.

Output power  $P$  can be calculated via voltage  $V$ .

$$P = \frac{V^2}{R_L} \quad (7)$$

Average power  $P_{ave}$  can be calculated via root mean square (rms) voltage  $V_{rms}$ .

$$P_{ave} = \frac{V_{rms}^2}{R_L} \quad (8)$$

Table 1. Dimensions and material properties of the prototype.

	Description	Value
Piezo stack	Density (kg/m <sup>3</sup> )	7700
	Piezoelectric charge constant $d_{33}$ (10 <sup>-12</sup> C/N)	710
	Coupling factor $K_{33}$	0.63
	Capacitance ( $\mu$ F)	5.76
	Material	Spring steel
Mechanical transformer	Density (kg/m <sup>3</sup> )	7850
	Young's modulus (GPa)	207
	Poisson's ratio	0.3
	Dimension (mm)	54×27×7
	Tilted angle	6°
Inertial mass	Mass (kg)	0.17
Magnet	Material	NdFeB
	Dimension (mm)	Ø20×10
	Density (kg/m <sup>3</sup> )	7500

### 3. EXPERIMENTS AND RESULTS

#### 3.1 Prototype fabrication and experiment setup

A prototype is fabricated based on the proposed architecture to test the energy harvesting performance as shown in Fig. 5. The mass system consists of a 0.17 kg inertial mass, a 0.025 kg magnet and a PLA plate spring designed to be at a resonant state at the excitation of 9 Hz. The piezo stack system comprises ferritic steel (11×7×6 mm) and a piezo stack transducer. A 560-layer piezoelectric stack (7×7×36 mm, Thorlabs) and a mechanical transformer made of spring steel and fabricated by electrical discharge machining are used to assemble the piezo stack transducer through an interference fit (Kuang et al., 2020). The detailed dimensions and material properties are summarized in Table 1.

Fig. 5 shows the experiment setup. The energy harvester is installed on an electromagnetic shaker (APS 113), which is actuated by the combination of a signal generator (Tektronix AFG3022C) and a power amplifier (APS125). The vibration generated by the shaker is measured by an accelerometer (Kistler 8762A5). The output of the energy harvester is connected to a variable load resistor. The voltage across the load resistor is measured to calculate the power output.

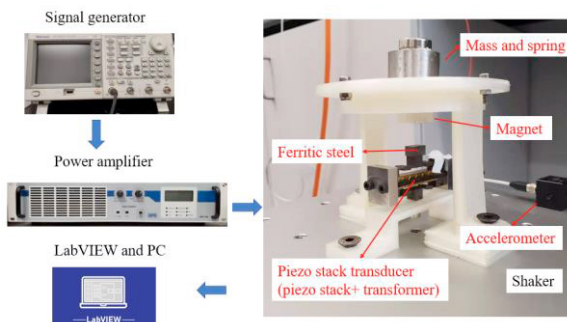
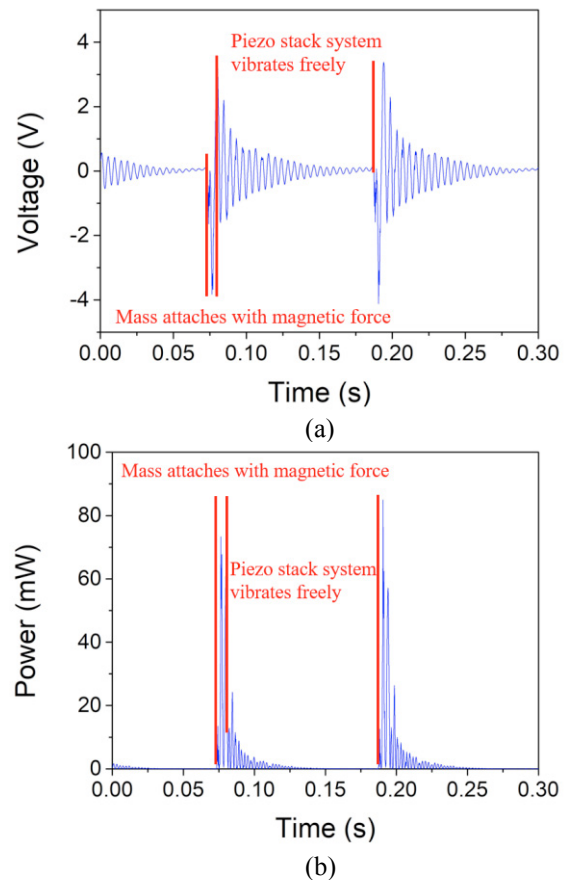


Fig. 5. Fabricated prototype and experimental setup

#### 3.2 Time-dependent response

First, we examine the energy harvester's time-dependent output voltage and power with a load resistor of 200  $\Omega$  at the excitation of 9 Hz and 1 g as shown in Fig. 6. The initial interval  $d_0$  is set to be 5 mm. The results show that the rms voltage is 0.649 V and the average power is 2.59 mW. It is noticed that at a resonant state, the mass system can attach and detach the piezo stack system frequently with large impact force, and thus the voltage and power are relatively high. Interestingly, the maximum voltage and power at each collision are different. This is because the change in the velocity of the piezo stack system is unique and variable at each collision. During each period, the energy harvester has two types of behaviour described in section 2 which can be observed in the voltage and power response. When the mass attaches and the two systems collide, the voltage changes from 0 to maximum in a very short period while the power reaches maximum accordingly. During this state, the mass system and piezo stack system vibrate together. When the mass detaches, the piezo stack system starts to vibrate freely at its resonance frequency, and the voltage decays gradually under the free vibration, and vast amounts of power are generated in this stage.

Fig. 6. The time-dependent output (a) voltage and (b) power of the energy harvester with a load resistor of 200  $\Omega$  at the excitation of 9 Hz and 1 g.



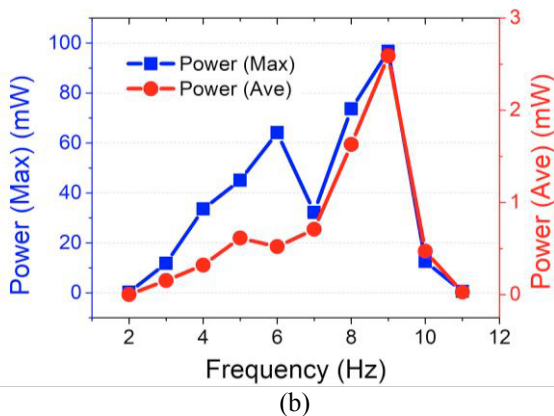
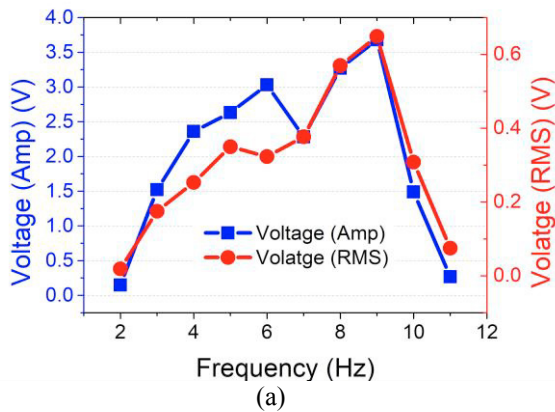


Fig. 7. The frequency response of the output (a) voltage (Amp- amplitude value, RMS- root mean square value) and (b) power (Max- maximum value, Ave- average value) of the energy harvester with a load resistor of  $200 \Omega$  at the excitation of  $1 g$  when the initial interval  $d_0$  is  $5 \text{ mm}$ .

### 3.3 Frequency response

After understanding the time-dependent response, we need to evaluate the frequency response. Fig. 7 shows the frequency response of the output voltage (Amp- amplitude value, RMS- root mean square value) and power (Max- maximum value, Ave- average value) of the energy harvester with a load resistor of  $200 \Omega$  at the excitation of  $1 g$  when the initial

interval  $d_0$  is  $5 \text{ mm}$ . When the excitation frequency (below  $4 \text{ Hz}$  and above  $11 \text{ Hz}$ ) is away from the natural frequency of the mass system, the piezo stack system cannot be attached to the mass system because of the small displacement of the mass system. As a result, the output voltage and power remain low. As the excitation frequency ( $5\text{-}7$  and  $10 \text{ Hz}$ ) is shifting towards the natural frequency, the displacement of the mass system increases, leading to the collision with the piezo stack system thanks to the attractive magnetic force and thus improved voltage and power output. When the excitation frequency equals the natural frequency ( $9 \text{ Hz}$ ), the mass system exerts a large impact force on the piezo stack system, and the output voltage and power reach the maximum. The amplitude and RMS values of the voltage are  $3.68 \text{ V}$  and  $0.649 \text{ V}$ , respectively, leading to a maximum power of  $96.69 \text{ mW}$  and average power of  $2.59 \text{ mW}$ . It is noticed that the

amplitude voltage and maximum power may be random at some point due to the uncertainty of the collision (for example at  $7 \text{ Hz}$ ), but the overall trend is the same as the change of the rms voltage and average power.

### 3.4 Impedance matching

Impedance matching is crucial to piezoelectric energy harvesting. Therefore, we obtain the output power against load resistance at the excitation of  $9 \text{ Hz}$  and  $1 g$  when the initial interval  $d_0$  is  $5 \text{ mm}$  as depicted in Fig. 8. The average power is used to select the optimum load resistance and as a result an external resistance of  $200 \Omega$  is chosen as the optimum value.

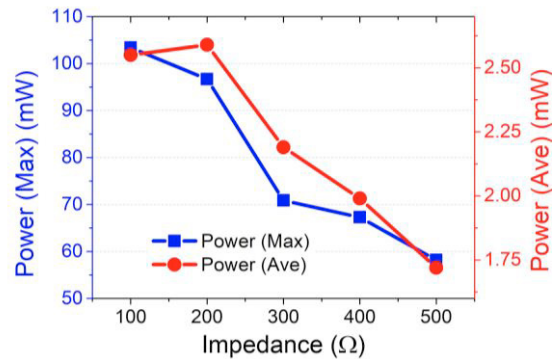


Fig. 8. Power output against load resistance at the excitation of  $9 \text{ Hz}$  and  $1 g$  when the initial interval  $d_0$  is  $5 \text{ mm}$ .

## 4. CONCLUSIONS

In this work, we proposed and experimentally validated a piezo stack energy harvester using the frequency up-conversion method achieved by an attractive magnetic force for harvesting energy from rail track vibration. For each period, the inertial mass attaches and then detaches the piezo stack transducer, allowing the piezo stack transducer to vibrate freely. In this way, the frequency up-conversion mechanism is implemented. The attractive magnetic force contributes to enabling the inertial mass to collide with the piezo stack transducer, especially when the excitation frequency is near the resonant frequency. A theoretical model of the proposed energy harvester considering the colliding motion and magnetic force is established. A prototype is fabricated and tested. Peak power of  $96.69 \text{ mW}$  and average power of  $2.59 \text{ mW}$  are achieved at an input acceleration of  $1 g$  applied at  $9 \text{ Hz}$  with an optimum load impedance of  $200 \Omega$ . The time-dependent responses, frequency responses and impedance are investigated to understand their influence on the energy harvesting performance.

## ACKNOWLEDGEMENTS

The authors would like to acknowledge the University of Exeter for financial support.

## REFERENCES

- BOSSO, N., MAGELLI, M. & ZAMPIERI, N. (2020). Application of low-power energy harvesting solutions in

- the railway field: a review. *Vehicle System Dynamics*, 1-31.
- BRADAI, S., NAIFAR, S., VIEHWEGER, C. & KANOUN, O. (2018). Electromagnetic Vibration Energy Harvesting for Railway Applications. *MATEC Web of Conferences*, 148.
- CAHILL, P., NUALLAIN, N. A. N., JACKSON, N., MATHEWSON, A., KAROUMI, R. & PAKRASHI, V. (2014). Energy Harvesting from Train-Induced Response in Bridges. *Journal of Bridge Engineering*, 19.
- CAO, L.-M., LI, Z.-X., GUO, C., LI, P.-P., MENG, X.-Q. & WANG, T.-M. (2019). Design and Test of the MEMS Coupled Piezoelectric–Electromagnetic Energy Harvester. *International Journal of Precision Engineering and Manufacturing*, 20, 673-686.
- CLEANTE, V. G., BRENNAN, M. J., GATTI, G. & THOMPSON, D. J. (2019). On the target frequency for harvesting energy from track vibrations due to passing trains. *Mechanical Systems and Signal Processing*, 114, 212-223.
- COVACI, C. & GONTEAN, A. (2020). Piezoelectric Energy Harvesting Solutions: A Review. *Sensors (Basel)*, 20.
- DE PASQUALE, G., SOMÀ, A. & ZAMPIERI, N. (2012). Design, Simulation, and Testing of Energy Harvesters With Magnetic Suspensions for the Generation of Electricity From Freight Train Vibrations. *Journal of Computational and Nonlinear Dynamics*, 7.
- FAN, K., LIU, S., LIU, H., ZHU, Y., WANG, W. & ZHANG, D. (2018). Scavenging energy from ultra-low frequency mechanical excitations through a bi-directional hybrid energy harvester. *Applied Energy*, 216, 8-20.
- GALCHEV, T. V., MCCULLAGH, J., PETERSON, R. L. & NAJAFI, K. (2011). Harvesting traffic-induced vibrations for structural health monitoring of bridges. *Journal of Micromechanics and Microengineering*, 21.
- GAO, M., WANG, P., CAO, Y., CHEN, R. & CAI, D. (2016a). Design and Verification of a Rail-Borne Energy Harvester for Powering Wireless Sensor Networks in the Railway Industry. *IEEE Transactions on Intelligent Transportation Systems*, 1-14.
- GAO, M. Y., WANG, P., CAO, Y., CHEN, R. & LIU, C. (2016b). A rail-borne piezoelectric transducer for energy harvesting of railway vibration. *Journal of Vibroengineering*, 18, 4647-4663.
- JIANG, H. & GAO, L. (2020). Study of the Vibration-Energy Properties of the CRTS-III Track Based on the Power Flow Method. *Symmetry*, 12.
- KUANG, Y., CHEW, Z. J. & ZHU, M. (2020). Strongly coupled piezoelectric energy harvesters: Finite element modelling and experimental validation. *Energy Conversion and Management*, 213.
- LIAO, W.-H., UNG, C., MOSS, S. D. & CHIU, W. K. (2015). Electromagnetic energy harvester using coupled oscillating system with 2-degree of freedom. *Active and Passive Smart Structures and Integrated Systems 2015*.
- NELSON, C. A., PLATT, S. R., ALBRECHT, D., KAMARAJUGADDA, V. & FATEH, M. (2008). Power harvesting for railroad track health monitoring using piezoelectric and inductive devices. *Active and Passive Smart Structures and Integrated Systems 2008*.
- PAN, Y., LIN, T., QIAN, F., LIU, C., YU, J., ZUO, J. & ZUO, L. (2019). Modeling and field-test of a compact electromagnetic energy harvester for railroad transportation. *Applied Energy*, 247, 309-321.
- SHENG, X., JONES, C. J. C. & THOMPSON, D. J. (2003). A comparison of a theoretical model for quasi-statically and dynamically induced environmental vibration from trains with measurements. *Journal of Sound and Vibration*, 267, 621-635.
- WANG, J., SHI, Z., XIANG, H. & SONG, G. (2015). Modeling on energy harvesting from a railway system using piezoelectric transducers. *Smart Materials and Structures*, 24.